Alexandria Engineering Journal (2020) 59, 3699–3707

HOSTED BY

Alexandria University

Alexandria Engineering Journal

www.elsevier.com/locate/aej
www.sciencedirect.com

A robust experimental-based artificial neural network approach for photovoltaic maximum power point identification considering electrical, thermal and meteorological impact

Samer Gowid [a,*], Ahmed Massoud [b]

[a] Department of Mechanical and Industrial Engineering, Qatar University, Qatar
[b] Department of Electrical Engineering, Qatar University, Qatar

Received 4 March 2020; revised 4 June 2020; accepted 5 June 2020
Available online 23 June 2020

KEYWORDS

Maximum power point;
Photovoltaic;
Solar panel;
Artificial intelligence;
Power generation;
Neural network

Abstract This paper aims to develop a robust and practical photovoltaic (PV) Maximum Power Point (MPP) identification tool developed using reliable experimental data sets. The correlations between the voltage and the current (V_{mp} and I_{mp}) at maximum power from one side, and the irradiance information, electrical parameters, thermal parameters and weather parameters from another side, are investigated and compared. A comparative study between a number of input scenarios is conducted to minimize the MPP estimation error. Four scenarios based on a combination of various PV parameters using various Artificial Neural Network (ANN)-based MPP identifiers are presented, evaluated using the most common regression measure (Mean Squared Error (MSE)), improved in terms of the accuracy of the identification of MPP, and then compared. The first scenario is divided into two parts I(a) and I(b) and considers the irradiance information in addition to the highest correlated parameters with I_{mp} and V_{mp}, which are circuit current (I_{sc}) and open-circuit voltage (V_{oc}), respectively. The second scenario considers irradiance information and the electrical parameters only. The irradiance information, in addition to the electrical, thermal, and weather parameters, are considered in the third scenario using a single layer network, while the irradiance information, in addition to the electrical, thermal, and weather parameters, are considered in the fourth scenario using a two-layer ANN network. Although the correlation study shows that the V_{mp} and I_{mp} have the best correlation with the open-circuit voltage and the short circuit current (scenario I), respectively. Nonetheless, the consideration of irradiance, electrical, thermal, and weather parameters (scenario IV) yielded higher identification accuracy. The results showed a decrease in the MSE of V_{mp} by 74.3% (from 1.6 V to 0.411 V), and in the MSE of I_{mp} by 95% (from 4.4e−6 A to 2.16e−7 A), respectively. In comparison to the conventional methods, the proposed concept outperforms their performances and dynamic responses. Moreover, it has

* Corresponding author.
E-mail addresses: samer@qu.edu.qa (S. Gowid), ahmed.massoud@qu.edu.qa (A. Massoud).
Peer review under responsibility of Faculty of Engineering, Alexandria University.

https://doi.org/10.1016/j.aej.2020.06.024

the potential to eliminate the oscillations around the MPP in cloudy days. The MPP prediction performance is 99.6%, and the dynamic response is 276 ms.

1. Introduction

Photovoltaic (PV) solar systems exist in different configurations for a broad range of applications such as grid-connected mode and isolated mode of operation. PV panels have non-linear relationships not only between voltage and current but also between their operating environmental conditions, panel characteristics, and their maximum power generation. This can be investigated using the well-known Current-versus Voltage (I-V) curve [1,2]. The non-linear behavior of solar panels can be represented primarily by the Fill Factor (FF), which is defined as the ratio between the maximum power produced by a solar panel to the product of open-circuit voltage (V_{oc}) and short-circuit current (I_{sc}). In general, FF, V_{oc}, and I_{sc} are the basic electrical parameters that can yield a convenient approximation for the electrical behavior of PV panels under typical operating conditions [3].

As the irradiance level varies during the day, the load characteristic, at which the power transfer is maximum, changes. To obtain the maximum power at any given environmental conditions, the electrical load characteristic should be adjusted to track the Maximum Power Point (MPP) on the Current-Versus-Voltage (I-V) characteristics of the PV system, where the Maximum Power Point Tracking (MPPT) is the process of identifying the MPP and maintaining the load operating point there all the time [3]. The MPPT approach is typically integrated with the power converter control [4–7]. Various MPPT techniques were developed to identify PV MPP. The conventional MPPT techniques are Perturb and Observe (P&O), Incremental Conductance (IncCond) [3,8,9].

A multilayer perceptron (MLP) is a dominant class of feed-forward ANN. It is commonly used for pattern recognition and function approximation (regression). MLP is made of, at least, three layers of neurons that utilize a nonlinear activation function. These three layers are (a) an input layer, (b) a hidden layer(s), and (c) an output layer. The Sigmoidal and Hyperbolic Tangent functions are of the most common ANN activation functions. The basic structure of the MLP is illustrated in Fig. 1. Backpropagation is a supervised learning technique, which is utilized for training MLP based networks. The multi-layer option and the nonlinear activation function are the options that make the MLP networkers different from linear perceptron networks [13].

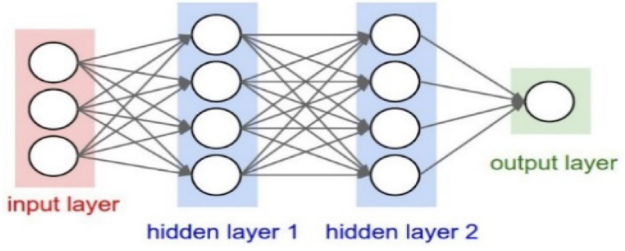

Fig. 1 Typical neural network architecture.

The most common performance evaluation function for regression problems is the Mean-Squared Error (MSE) [13–15], and it is used in this study to assess the prediction performance of the proposed network configurations. There are numerous types of ANN learning algorithms in the literature. However, it is challenging to identify which of these training algorithms would be the most suitable for a given problem in terms of accuracy. Based on the results of various experiments, MLP is an effective ANN architecture, and the Levenberg-Marquardt (LM) is one of the most accurate ANN training algorithms as it can obtain the lowest MSE when employed to solve various function approximation problems [15]. On the other hand, the Scaled Conjugate Gradient (SCG) algorithm also provides good performance over a wide variety of function approximation problems.

The LM algorithm is defined as an iterative technique, which locates a local minimum of multivariate functions. These functions are expressed as the sum of squares of several non-linear and real-valued functions, while the SCG is a second-order conjugate gradient algorithm that is developed to accelerate and improve the identification of the global minimum of multivariate functions [12,15].

ANN-based MPPT may be used as the main MPPT approach [20–29]. On another frontier, ANN-based MPPT may be combined as an auxiliary MPPT technique with one of the Artificial Intelligence MPPT techniques, such as Fuzzy Logic Controller. Moreover, ANN-based MPPT techniques can be classified based on the controller input type. The major three types are (a) electrical inputs only (short-circuit current (I_{SC}) and open-circuit voltage (V_{OC})), (b) non-electrical inputs only (irradiance (G) and temperature (T)), and (c) combined electrical and non-electrical inputs. The majority of researches considered a single type only, while a few of them considered a combination of electrical and non-electrical input types [12].

It can be observed that the parameter combination scenarios are limited in the literature and need further investigation, to maximize the accuracy of the MPP identification using a good combination of parameters as well as a proper configuration of an ANN architecture. To the best knowledge of the authors, the combination of the fill factor, relative humidity, atmospheric pressure, and surface temperature of the PV panel have not been considered, and their effect on the overall performance of the ANN-based MPPT controller has not been addressed before, which will be pinpointed in this paper. Fig. 2 illustrates the research methodology employed in this study.

Therefore, among a large number of ANN-based PV MPPT techniques, the following approaches have not been investigated thoroughly:

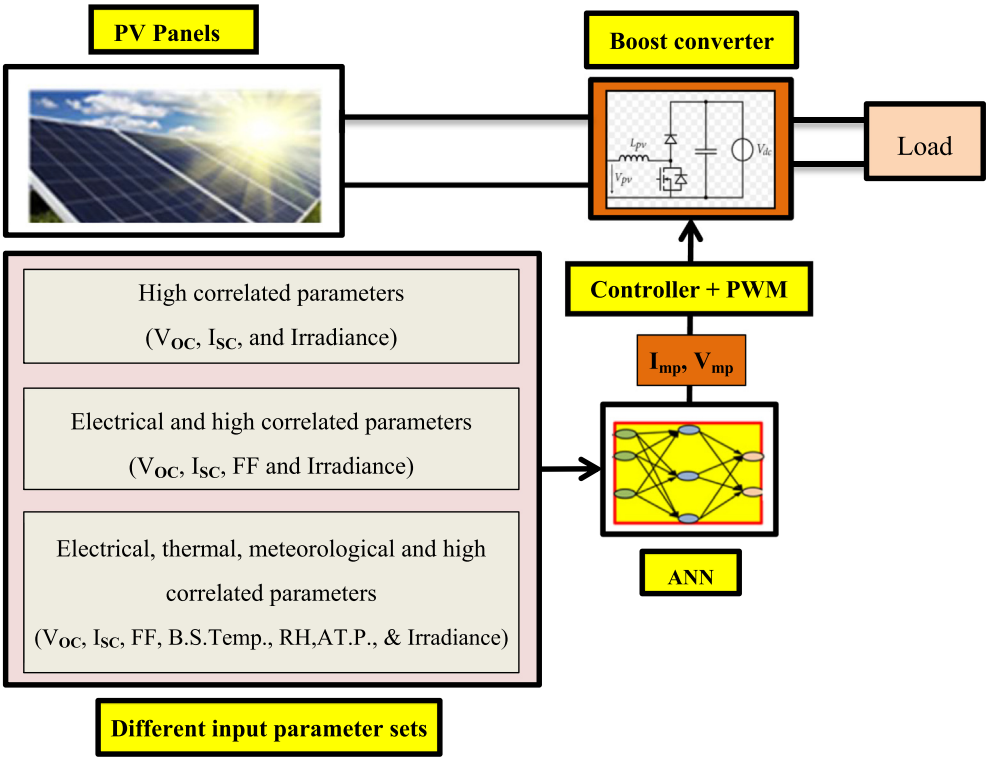

Fig. 2 The methodology of the comparative study.

(a) The correlation between a large number of PV parameters, including the electrical, thermal, and meteorological parameters on the one hand and the MPP parameters, on the other hand.
(b) The impact of the combination of these parameters on the prediction accuracy of ANN-based solutions based on the correlation as well as by using trial and error method. The prediction results are significantly affected by the input parameters combination, and, unlike the previous work, this paper considers a large number of different PV parameters.

The P&O technique has the following disadvantages: (a) power oscillations at steady-state operation around the MPP, (b) slow convergence, and (c) inaccurate MPP determination in cloudy days [10]. While the incremental conductance technique is more accurate then P&O as it can determine the MPP without oscillating around it, however, it requires heavy computation in the controller, fast power slope calculation as well as a high sampling rate. This adversely affects its transient performance producing oscillations when operating conditions change rapidly [11]. Moreover, the majority of the introduced methods employ a limited number of PV parameters, in particular, electrical parameters, which hinder the efforts to investigate the effect of other non-electrical parameters on the MPP identification accuracy. Thus, this work will not only consider the electrical parameters but also will be extended to consider the thermal and meteorological parameters that affect the non-linear internal resistance of a PV panel. These parameters variably affect the load resistance for MPP, increase the complexity, and affect the performance of the aforementioned MPPT approaches.

Although the major conventional MPPT techniques provide acceptable performance, Artificial Neural Network (ANN)-based MPPT techniques demonstrated faster and more accurate MPP identification results, particularly when considering partial shading or fast environmental changes. This comes in agreement with the strength of ANN in solving non-linear problems [3,9]. ANN-based PV MPPT methods have been addressed extensively in the literature, and ANN algorithms demonstrated a number of capabilities such as (a) non-linear mapping, (b) fast response, (c) reliable and stable operation, (d) compact and accurate solution for multi-variable problems, (e) off-line training and (f) reduced computational burden [12].

Thus, in this context, the main contribution of the paper can be summarized in the following bullets:

- Investigate the correlation between the voltage and current at maximum PV power on the one hand, and the electrical, thermal, and weather parameters, on the other hand.
- Develop, compare, and evaluate the performance of a set of experimental ANN models for MPP detection at various working conditions, including cloudy days to overcome the drawbacks of the conventional MPPT methods as well as to improve the MPP identification performance. The experimental networks will consider the correlation results as well as other parameters combination scenarios. This is carried out using accurate and reliable experimental data collected by the National Renewable Energy Laboratory, U.S. Department of Energy, USA [16].

This paper is divided into 5 sections. Section 1 presents the introduction, literature review, and the scope of this work.

Sections 2 explains the mathematical model of PV arrays and delivers information about the experimental data sets used in this study. The correlations between different PV parameters are investigated and identified in the same section. In Section 3, the performances of improved conventional MPPT methods are discussed and summarized. Various ANN models based on several parameter combinations and ANN configuration scenarios are introduced, investigated, and evaluated for their MPP identification performance in Section 4. Finally, the results of this study are summarized in Section 5.

2. Correlation between I_{mp} and V_{mp} with PV electrical, thermal, and meteorological parameters

This section provides the mathematical model along with the parameters that influence the power generation of PV arrays. Also, it provides the correlation relationships between MPP parameters and various PV parameters. The PV cell equivalent circuit is shown in Fig. 3. The voltage-current characteristic equations of a solar PV cell are given in (1)–(3).

$$I = I_{ph} - I_s\left(e^{\frac{q(V+IR_s)}{KATc}}\right) - \frac{V + IR_s}{R_{sh}} \tag{1}$$

$$I_{ph} = G[I_{sc} + K_I(T_c - T_{ref})] \tag{2}$$

$$I_S = I_{rs}\left[\frac{T_c}{T_{ref}}\right]^3 e^{\frac{qEg(T_c - T_{ref})}{T_{ref}T_cKA}} \tag{3}$$

where I: Solar cell current (A), V: Solar cell voltage (V), I_{ph}: Light generated current (A), I_s: Cell saturation current (A), q: Electron charge; $1.602\text{x}10^{-19}$ J/V, R_s: Series resistance (Ω), R_{sh}: Shunt resistance (Ω), K: Boltzmann's constant; $1.38\text{x}10^{-23}$ J/K, A: Diode ideality factor, T_C: Cell temperature (K), and G: Insolation (W/m^2). I_{SC}: Cell's short-circuit current at 298 K and 1 kW/m^2, T_{ref}: Reference temperature of the cell; 298 K, and K_I: Short circuit temperature coefficient; 0.0017 (A/°C). I_{rs}: Cell's reverse saturation current at a reference temperature and solar radiation, and E_g: Band-gap energy.

The correlation study presented in this paper is based on experimental data sets. These data sets were collected by the National Renewable Energy Laboratory, U.S. Department of Energy, USA. The data were recorded for one year at three climatically diverse locations (Cocoa, Florida; Eugene, Oregon; and Golden, Colorado) and for PV modules representing all technologies available in 2010 when the work began [16]. The different types of PV modules are shown in Fig. 4. This study utilizes the experimental data provided about the Amorphous Silicon/ Microcrystalline Silicon PV panel (Model H). The panels were deployed at Coca, Florida, in 2010. The data sets contain data for an entire year, including cloudy days.

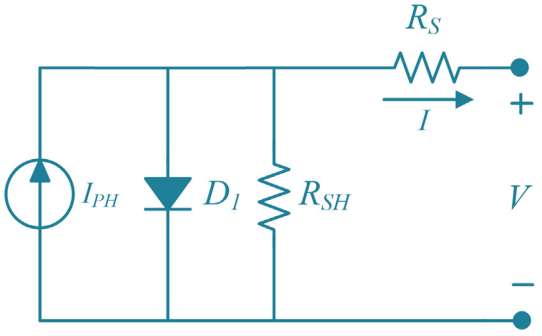

Fig. 3 PV cell equivalent circuit diagram.

Regression analysis is performed to identify the highly correlated parameters with I_{mp} and V_{mp}. The parameters considered in this correlation study are:

- The back surface temperature of the PV panel (B.S.Temp).
- Short circuit current (I_{sc}).
- Open circuit voltage (V_{oc}).
- Fill Factor (FF) that reflects the quality of the solar cell.
- The meteorological information; namely Relative Humidity (RH) and Atmospheric Pressure (AT. P.).

The degree of relationship in the patterns of variation of input X_a and output Y_b variables is calculated through the calculation of Pearson's linear correlation coefficient (ρ). ρ can be calculated as follows [17,18].

$$\rho(a,b) = \frac{\sum_{i=1}^{n}\left(X_{a,i} - \overline{X}_a\right)\left(Y_{b,i} - \overline{Y}_b\right)}{\left\{\sum_{i=1}^{n}\left(X_{a,i} - \overline{X}_a\right)^2\sum_{j=1}^{n}\left(Y_{b,j} - \overline{Y}_b\right)^2\right\}^{1/2}} \tag{4}$$

$$\overline{X}_a = \sum_{i=1}^{n}(X_{a,i})/n \;\; and \;\; \overline{Y}_b = \sum_{j=1}^{n}\left(Y_{b,j}\right)/n \tag{5}$$

where n is the length of each column.

The value of ρ varies between "1″ for perfect correlation, and "-1" for the perfect negative correlation. While zero correlation means that the variation of one variable cannot be employed to explain the variation in the other variable. Table 1 shows the results of the regression analysis. It displays a matrix of the pairwise linear correlation coefficient between the output parameters (I_{mp} and V_{mp}) and the input parameters (irradiance, B.S.Temp, I_{sc}, V_{oc}, FF, RH, and AT.P.). I_{mp} was found in a good correlation with I_{sc} and Irradiance, while V_{mp} was found in a good correlation with V_{oc} and irradiance (the two highest correlated parameters).

3. Performance of improved conventional MPPT methods

Tan et al. [30] conducted various experiments to improve the performance of MPP identification using the Perturb and Observe technique. The results showed that 99.25% performance could be achieved when using a variable step-size algorithm applied to a Cascaded Multilevel Converter (CMC) converter and that the performance remained unchanged with the variation of solar irradiance. Yilmaz et al. [31] proposed a new MPPT method with a 99.5% minimum performance. This method is based on the calculation of the reference voltage using the Fuzzy Logic technique to adjust the PWM duty cycle that controls the output of a DC-DC converter. Yang and Wen [32] managed to improve the dynamic response of the conventional Perturb and Observe (P&O) technique using a variable and adaptive (P&O) method with current predictive control. The results showed that the oscillations were reduced and that the dynamic response was improved by 23.3%, lowered from 9.92 s to 7.6 s in cloudy days (considerable variation in V_{mp}). Support Vector Machine (SVM) technique was also employed to improve the identification accuracy of MPP [33]. The results showed that the proposed method yielded

Fig. 4 PV modules deployed at the National Renewable Energy Laboratory [16].

Table 1 Coefficients of correlation (ρ) between output and input PV variables.

	I_{mp}	V_{mp}
Irradiance	0.998455	0.540097
B.S.Temp.	0.8471	0.272529
I_{sc}	0.999936	0.520085
V_{oc}	0.698083	0.955706
FF	−0.272	0.144094
RH	−0.03582	−0.15133
AT. P.	−0.02822	−0.14822

an RMSE of 0.71 V and a performance of 96% (accuracy per sample), given that the maximum voltage of the panel is 18 V only. However, the method was tested using a limited number of data sets, and the dynamic response is not reported.

Padmanaban et al. [34] presented a Modified Sine-Cosine Optimized (MSCO) maximum power point tracking algorithm for grid integration. The authors demonstrated improved performance when compared to the performances of the classical Particle Swarm Optimization (PSO) and Artificial Bee Colony (ABC) algorithms (see Table 2).

Silva et al. [35] proposed the implementation of a Feed-Forward Control Loop (FFCL) to enhance the dynamic response of double-stage single-phase grid-tied PV systems subjected to sudden solar radiation changes, like in cloudy days. The results shown in Table 3 demonstrate that the proposed technique yielded a better performance and dynamic response as it managed to improve the performance by reducing the overshoot to 4.3% and the dynamic response to 0.6 s.

In summary, various researches have been performed to improve the drawbacks of the conventional MPPT methods. Based on the reviewed work, it can be observed that the best-reported performance is 99.5%, and this could be achieved by using a Fuzzy Logic controller. However, the reliability of the reported results should be improved, as the authors utilized a limited number of data sets in the evaluation process. The dynamic response of the improved conventional MPP identification process was also improved, reaching 0.6 s. It can also be observed that the main drawback of the hill-climbing conventional methods, which is the oscillations around the MPP, particularly in cloudy days, still exists. The results of this study are compared with the performances of the conventional and improved MPP methods reported in this section.

Table 2 Performance comparison of MPP tracking algorithms [34].

Method	Average performance
PSO	94.63
ABC	97.13
MSCO	98.40

Table 3 Performance improvement using FFCL technique [35].

Technique	P&O	PSO	P&O	PSO
FFCL	No	No	Yes	Yes
Settling time (s)	0.9	2.7	0.6	1.2
Overshoot (%)	47.8	39.1	4.3	4.3

4. MPP prediction using ANN

The most popular and well-proven ANN architecture, training algorithm, and error calculation method utilized for function approximation are employed to carry out this comparative study. MLP architecture is utilized in combination with the SCG and LM supervised learning algorithms. The performance of the network is evaluated using the MSE quantitative measure at different neurons and hidden layer configurations. Four ANN configuration scenarios are studied in this paper (see Table 4), namely:

(a) The first scenario (divided into two parts I(a) and I(b)) considers the irradiance information in addition to the highest correlated parameters with I_{mp} and V_{mp}, which are I_{sc} and V_{oc}, respectively.
(b) The second scenario considers irradiance information and the electrical parameters only.
(c) The irradiance information, in addition to the electrical, thermal, and weather parameters, are considered in the third scenario using a single layer network.

Table 4 Scenarios of the development of ANN networks.

Scenario	Parameters	Output(s)	ANN
I(a)	Irradiance and V_{oc}	V_{mp}	Single-layer LM trained network
I(b)	Irradiance and I_{sc}	I_{mp}	Single-layer LM trained network
II	Irradiance, V_{oc}, I_{sc} & FF	I_{mp} and V_{mp}	Single-layer LM trained network
III	Irradiance, V_{oc}, I_{sc}, FF, B.S. Temp, At. Pressure & RH	I_{mp} and V_{mp}	Single-layer SCG & LM trained network
IV	Irradiance, V_{oc}, I_{sc}, FF, B.S. Temp, At. Pressure & RH.	I_{mp} and V_{mp}	Two-layered LM trained network

(d) The irradiance information, in addition to the electrical, thermal, and weather parameters, are considered in the fourth scenario using a two-layer network.

In the first three scenarios, a single-layered ANN configuration (a single hidden layer only) is addressed, and the near-optimal node number is decided by trial and error method. The number of nodes ranges from 2 nodes to 60 nodes. While the fourth scenario investigates the effect of increasing the hidden layer number on the accuracy of the most accurate network (two-layered network). Due to the difference between the output parameters (i.e., current and voltage), it was imperative to carry out data normalization (or standardization), so that the data points to be within uniform scale range prior to any training or testing. The normalization is carried out within the uniform scale range for each of the two output signals. The normalization process ensures a better fit and helps to prevent the training from diverging. This standardization process results in training data with zero mean and a unity variance [19].

Six supervised neural network models are developed based on the four parameters combinations and ANN configuration scenarios shown in Table 4. The best scenario and ANN architecture are selected based on the results of the comparative study shown in Table 5, where the MPP identification performance of all of the network options is evaluated.

Due to the importance and significance of the irradiance information, it is considered as an essential parameter in all of the ANN models. A total of 12,149 data sets related to amorphous silicon/ microcrystalline silicon PV panel (model H) were utilized for the training, validation, and testing of the proposed ANN models; 70% for training and 30% for validation and testing.

For the first scenario (I (a) & I (b)), near-optimal neural network configurations are identified by trial and error method considering a single-layered neural network with 2 nodes to 60 nodes per layer. The results favored the utilization of an ANN configuration of 38 nodes, trained using the LM algorithm, as it yielded an MSE (I_{mp}) and MSE (V_{mp}) of as low as 0.4A and 1.6 V, respectively. More input parameters are incorporated to investigate the possibility of further improvement in the achieved results (Scenario II). These parameters are the three electrical parameters in addition to the irradiance information. The improved ANN model yielded a better overall MSE value of 0.229, MSE (I_{mp}), and MSE (V_{mp}) values of 2.5e−7A and 0.541 V, respectively. Next, more comprehensive sets that include electrical, weather, and thermal parameters are considered to investigate their effect on MPP identification performance.

The results showed that the latter scenario provided more accuracy over the other addressed scenarios. Therefore, to investigate the effect of the second popular training algorithm on the MPP identification accuracy, the same input parameters were utilized to develop a single-layered ANN model that was trained using the SCG algorithm (Scenario III). The results demonstrate that the LM training algorithm gives better

Table 5 MSE across the training points for the proposed ANN configurations.

	Scenario I		Scenario II	Scenario III		Scenario IV
Number of Inputs	2 inputs **(I_a)**	2 inputs **(I_b)**	4 inputs	7 inputs		7 inputs
Number of layers	Single	Single	Single	Single	Single	Two
Training algorithm	LM	LM	LM	SCG	LM	LM
Number of nodes	38	38	33	39	18	35–35
MSE (I_{mp} + V_{mp})	0.4	1.63	0.229	0.544	0.186	0.115
MSE (I_{mp})	4.4e−6	–	2.5e−7	2.1e−6	2.6e−7	2.16e−7
MSE (V_{mp})	–	1.60	0.541	0.91	0.427	0.411

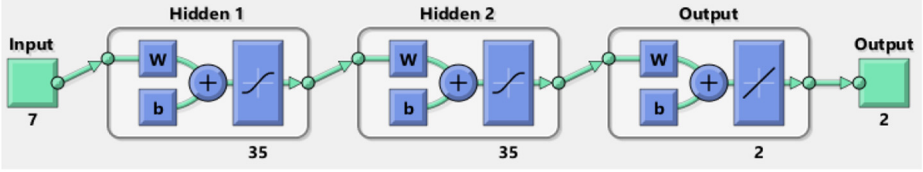

Fig. 5 The architecture of the neural network with the most accurate results.

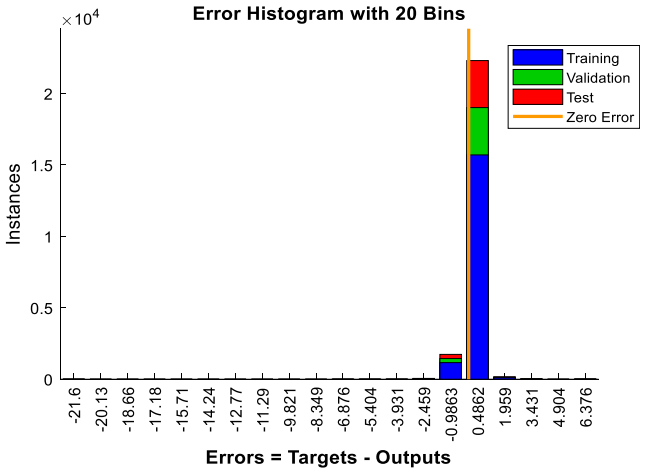

Fig. 6 Error histogram of a two hidden layers network with 35 nodes each.

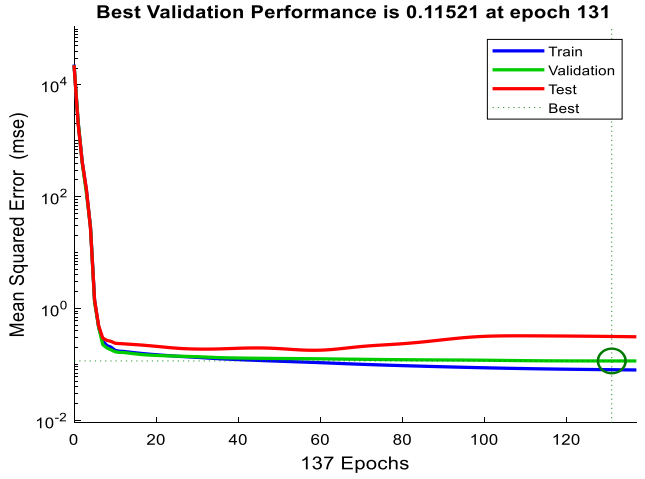

Fig. 7 MSE of the best network model.

results. Thus, the LM trained model is considered for further improvement through the investigation of the performance of a two-layered ANN model.

The results reveal that a two-layered neural network, trained using the LM algorithm, with 35 nodes per each layer, yields an identification accuracy of as low as 2.16e−7 A for I_{mp} and 0.411 V for V_{mp}. The configuration of the best ANN is shown in Fig. 5, and Fig. 6 depicts the error histogram of the neural network. It can be observed that the vast majority of the predicted results are very close to Zero Error and that the prediction accuracy using the validation and testing data sets are very close to the training data set. Fig. 7 shows the MSE values for the training, validation, and testing data sets.

The performance of the three major scenarios was re-evaluated using the validation and testing data sets only, given that these data sets were not used for training. The error values between the experimental and predicated I_{mp} and V_{mp} values, along with their MSE values, are presented in Tables 6 and 7. The values provided in both tables are based on 3,644 data sets, which represent 30% of the total number of data sets, which the network was not trained for. The MSE values for

Table 6 Samples of The current error for maximum power and the MSE values for 3644 points (training data sets excluded).

S	Scenario I	Scenario II	Scenario IV
1	7.59296E−05	−0.000180972	0.0001809724
2	0.000551884	−0.000234894	0.0002348944
3	0.000482563	−5.13366E−05	0.0000513366
4	0.000900787	−2.14501E−05	0.0000214501
5	−0.000727202	−8.60215E−05	0.0000860215
6	0.000878776	0.000205323	−0.0002053227
7	0.000516021	−9.87946E−05	0.0000987946
8	0.000443478	0.000103108	−0.0001031079
9	0.000367478	0.000259074	−0.0002590738
10	0.000273192	−9.6786E−05	0.0000967860
...			
...			
3635	0.0023392011	−0.0007630250	−0.0000886039
3636	0.0028326705	−0.0005146894	−0.0001388747
3637	0.0027477459	−0.0006504482	0.0000370465
3638	0.0021374672	−0.0005386899	0.0000157155
3639	0.002405071	−0.000258079	−1.16437E−06
3640	0.002175054	−0.00023125	−0.000134678
3641	0.002215853	−0.000134343	−0.000316017
3642	0.000874619	−0.000567427	−0.000253311
3643	0.000239029	−0.000204717	−0.0001237
3644	1.81451E−05	−0.000404709	−0.000116551
MSE	0.002100214	0.000500584	0.00046484

Table 7 Samples of the voltage error in voltage for maximum power and the MSE values for 3644 points (training data sets excluded).

S	Scenario I	Scenario II	Scenario IV
1	−0.315682398	0.080088797	0.5089664399
2	0.792194143	0.33575908	0.1555556258
3	0.072142446	0.365742399	−0.0848434944
4	1.678976533	0.437869104	−0.1793745477
5	0.262960693	0.41761099	0.3625636701
6	1.625984023	0.048632379	0.0407990771
7	0.682766561	0.084234265	0.0348331697
8	0.174077534	0.030091712	−0.1903545549
9	0.833287455	0.347491104	−0.1435572542
10	0.559585086	1.752304009	−0.3394664499
...			
...			
3635	0.3519796918	0.2556361102	0.0344177713
3636	0.0486194993	0.2110844636	0.0899433344
3637	0.0704423213	0.2987839416	−0.0859520088
3638	−0.0002262156	0.2847134232	−0.0218535078
3639	−0.0139322	0.171866152	−0.225077031
3640	−0.071487996	0.125900627	−0.461139559
3641	0.07571133	−0.014985689	0.33900374
3642	−0.036736199	0.250141462	0.493316299
3643	−0.394013485	−0.003182016	−0.339584519
3644	−0.401909547	0.244218224	−1.274276248
MSE	1.268193694	0.73591758	0.641528513

I_{mp} and V_{mp} are 0.00046484 A and 0.641528513 V, respectively. These values are higher than the training MSE values, which are 2.16e-7 A and 0.411 V, respectively. The average

computer processing time required for the prediction of MPP is 276 ms using a DELL OPTIPLEX 7440 AIO machine (Core I7-6700 CPU @ 3.4 GHz (8CPUs) processor with 8 GB memory).

Knowing that the maximum V_{mp} in all experiments is 190 V and that the errors did not exceed 0.8 V (MSE of 0.64 V), this gives an MPP prediction performance of 99.6% (P = max. error/max. V_{mp}). Despite the difference between the training MSE values, and the validation and testing MSE values, the error values are still relatively small and hence lead to an MPP identification with reasonable accuracy. The performance of the proposed ANN network using this particular set of input parameters outperforms the best dynamic response and performance reported in Section 3, as it yields an MPP prediction performance of 99.6% and a dynamic response of 276 ms only in comparison to 99.5% and 0.6 s, respectively (see Section 3). The proposed network has the potential to eliminate the main drawback of hill-climbing techniques, which is the oscillations during cloudy days, as well as the slow dynamic response.

5. Conclusion

This paper aimed to develop a reliable practical ANN-based MPP identification tool that can be utilized to maximize the efficiency of PV panels. The prediction accuracy of MPP is influenced by the number, type, and combination of the different PV parameters in addition to the tool utilized for prediction. Thus, unlike the previous work, this paper considered a large number of PV input parameters with different combination scenarios to investigate their influence on the MPP prediction accuracy. ANN-based models are employed due to their dynamic, fast, and precise performance. Thus, ANN-MPPT models have the potential to consider variations in atmospheric and operating conditions in general. Training, validation, and testing of the proposed ANN models were carried out using sets of reliable experimental data collected by the National Renewable Energy Laboratory, U.S. Department of Energy. Six ANN-based MPP identification models with different input PV parameters were introduced and then evaluated for their performance. Two input parameters for the first two models were selected based on the highest correlated parameter in addition to the irradiance information. Four input parameters for the third model were incorporated to consider the irradiance information along with the three basic electrical parameters (V_{oc}, $I_{sc,}$ and FF). For the remaining ANN models, seven input parameters were carefully selected to represent the irradiance, weather, thermal and electrical parameters (V_{oc}, I_{sc}, FF, RH, atmospheric pressure, PV back surface temperature, and Irradiance information) to improve their identification accuracy further.

The results showed that, although the MPP is highly correlated with the open-circuit voltage and the short circuit current (scenario I), the consideration of irradiance, electrical, thermal, and weather parameters (scenario IV) yielded a higher MPP identification accuracy. The comparison results between both scenarios showed that the incorporation of all parameters decreased the MSE (V_{mp}) from 1.6 V to 0.411 V and the MSE (Imp) from 4.4 e−6 A to 2.16e−7 A, respectively. Moreover, with respect to the ANN configuration, the utilization of a two-layered neural network introduced in scenario IV is favored as it produced a higher prediction accuracy than the single-layered network introduced in scenario III (refer to Table 2 and Table 3). The comparison results between both scenarios showed that the utilization of a more deep network decreased the MSE (V_{mp}) from 0.427 V to 0.411 V and the MSE (Imp) from 2.6 e to 7 A to 2.16e-7 A, respectively. The performance of the proposed AI-based method outperforms the best dynamic response and performances reported in Section 3 and shown in Fig. 8, as it produces an MPP prediction performance of 99.6% and a dynamic response of 276 ms only in comparison to 99.5% and 0.6 s. Furthermore, the proposed method has the potential to eliminate the main drawbacks of the hill-climbing techniques, which are the oscillations during cloudy days and the slow dynamic response. The results of this study are limited to similar PV panels and, in particular amorphous silicon/ microcrystalline silicon – model H - PV panels. It is also limited to similar electrical, thermal, and meteorological conditions (the experimental conditions).

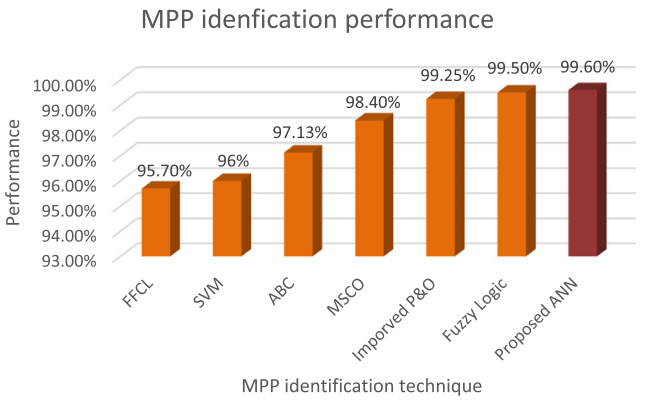

Fig. 8 Performance of different MPP identification techniques [30-35].

Declaration of Competing Interest

The authors declare that they have no known competing financial interests or personal relationships that could have appeared to influence the work reported in this paper.

Acknowledgements

The publication of this article was funded by the Qatar National Library.

References

[1] M.A.G. de Brito, L. Galotto, L.P. Sampaio, G.d.A. e Melo, C. A. Canesin, Evaluation of the Main MPPT Techniques for Photovoltaic Applications, in: IEEE Transactions on Industrial Electronics, vol. 60, no. 3, 2013, pp. 1156–1167.

[2] Y. Ji, D. Jung, J. Kim, J. Kim, T. Lee, C. Won, A real maximum power point tracking method for mismatching compensation in PV array under partially shaded conditions, IEEE Trans. Power Electron. 26 (4) (2011) 1001–1009.

[3] H. Wang, J. Shen, An improved model combining evolutionary algorithm and neural networks for PV maximum power point tracking, IEEE Access 7 (2019) 2823–2827.

[4] T. Esram, P.L. Chapman, Comparison of photovoltaic array maximum power point tracking techniques, IEEE Trans. Energy Convers. 22 (2) (2007) 439–449.
[5] E. Koutroulis, K. Kalaitzakis, N.C. Voulgaris, Development of a microcontroller-based, photovoltaic maximum power point tracking control system, IEEE Trans. Power Electron. 16 (1) (Jan. 2001) 46–54.
[6] S. Alghuwainem, Matching of a DC motor to a photovoltaic generator using a step-up converter with a current locked loop, IEEE Trans. Energy Convers. 9 (1994) 192–198.
[7] J.H.R. Enslin, M.S. Wolf, D.B. Snyman, W. Swiegers, Integrated photovoltaic maximum power point tracking converter, IEEE Trans. Ind. Electron. 44 (6) (Dec. 1997) 769–773.
[8] A.K. Abdelsalam, A.M. Massoud, S. Ahmed, P.N. Enjeti, High-performance adaptive perturb and observe MPPT technique for photovoltaic-based microgrids, IEEE Trans. Power Electron. 26 (4) (April 2011) 1010–1021.
[9] N. Femia, G. Petrone, G. Spagnuolo, M. Vitelli, A technique for improving P&O MPPT performances of double-stage grid-connected photovoltaic systems, IEEE Trans. Ind. Electron. 56 (11) (Nov. 2009) 4473–4482.
[10] M. Seyedmahmoudian, T.K. Soon, B. Horan, A. Ghandhari, S. Mekhilef, A. Stojcevski, New ARMO-based MPPT technique to minimize tracking time and fluctuation at output of PV systems under rapidly changing shading conditions, IEEE Trans. Ind. Inf. (2018), https://doi.org/10.1109/TII.2019.2895066.
[11] A. Chermitti, O. Hacene, B. Mohamed, Improvement of the "Perturb and Observe" MPPT algorithm in a photovoltaic system under rapidly changing climatic conditions, Int. J. Comput. Appl. 56 (12) (Oct. 2012) 5–10.
[12] L. Elobaid, A. Abdelsalam, E. Zakzouk, Artificial neural network-based photovoltaic maximum power point tracking techniques: a survey, IET Renew. Power Gener. 9 (8) (2015) 1043–1063.
[13] S. Gowid, R. Dixon, S. Ghani, Performance comparison between fast Fourier transform-based segmentation, feature selection, and fault identification algorithm and neural network for the condition monitoring of centrifugal equipment and neural network for the condition monitoring of Cen, J. Dyn. Syst., Meas., Control, Trans. ASME 139 (6) (2017), https://doi.org/10.1115/1.4035458.
[14] M.C. Di Piazza, M. Pucci, Induction-Machines-Based Wind Generators With Neural Maximum Power Point Tracking and Minimum Losses Techniques, IEEE Trans. Ind. Electron. 63 (2) (Feb. 2016) 944–955.
[15] MathWorks, "Choose a Multilayer Neural Network Training Function," MATLAB, [Online]. Available: https://www.mathworks.com/help/deeplearning/ug/choose-a-multilayer-neural-network-training-function.html. [Accessed 4/2019].
[16] B. Marion et al., New data set for validating PV module performance models, in: 2014 IEEE 40th Photovoltaic Specialist Conference (PVSC), Denver, CO, 2014, pp. 1362–1366.
[17] M.A.S. Masoum, H. Dehbonei, E.F. Fuchs, Theoretical and experimental analyses of photovoltaic systems with voltage and current-based maximum power-point tracking, IEEE Trans. Energy Convers. 17 (4) (Dec. 2002) 514–522.
[18] G. Garson, Correlation, Statistical Associates, 2013 edition, ASIN: B007VCSG6K, 2012.
[19] MATLAB, "Time Series Forecasting Using Deep Learning," Mathworks, [Online]. Available: https://www.mathworks.com/help/deeplearning/examples/time-series-forecasting-using-deep-learning.html. [Accessed 4/2019].
[20] W. Lin, C. Hong, C. Chen, Neural-Network-Based MPPT Control of a Stand-Alone Hybrid Power Generation System, IEEE Trans. Power Electron. 26 (12) (2011) 3571–3581.
[21] Y. Sun, S. Li, B. Lin, X. Fu, M. Ramezani, I. Jaithwa, Artificial neural network for control and grid integration of residential solar photovoltaic systems, IEEE Trans. Sustain. Energy 8 (4) (2017) 1484–1495.
[22] F. Lin, K. Lu, B. Yang, Recurrent fuzzy cerebellar model articulation neural network based power control of a single-stage three-phase grid-connected photovoltaic system during grid faults, IEEE Trans. Ind. Electron. 64 (2) (2017) 1258–1268.
[23] Syafaruddin, E. Karatepe, T. Hiyama, Artificial neural network-polar coordinated fuzzy controller based maximum power point tracking control under partially shaded conditions, IET Renew. Power Gener. 3 (2) (2009) 239–253.
[24] H.M. El-Helw, A. Magdy, M.I. Marei, A hybrid maximum power point tracking technique for partially shaded photovoltaic arrays, IEEE Access 5 (2017) 11900–11908.
[25] Y. Zhu, J. Fei, Adaptive global fast terminal sliding mode control of grid-connected photovoltaic system using fuzzy neural network approach, IEEE Access 5 (2017) 9476–9484.
[26] N. Kumar, B. Singh, B.K. Panigrahi, PNKLMF-based neural network control and learning-based HC MPPT technique for multiobjective grid integrated solar PV based distributed generating system, IEEE Trans. Ind. Inf. 15 (6) (2019) 3732–3742.
[27] Z. Yan, C. Li, Z. Song, L. Xiong, C. Luo, An improved brain storming optimization algorithm for estimating parameters of photovoltaic models, IEEE Access (2019), https://doi.org/10.1109/ACCESS.2019. 2922327.
[28] L. Du, L. Zhang, X. Tian, Deep power forecasting model for building attached photovoltaic system, IEEE Access 6 (2018) 52639–52651.
[29] S. Samara, E. Natsheh, Intelligent real-time photovoltaic panel monitoring system using artificial neural networks, IEEE Access 7 (2019) 50287–50299.
[30] C. Tan, T. Green, C. Aramburo, Analysis of perturb and observe maximum power point tracking algorithm for photovoltaic applications, in: Power and Energy Conference, 2008 (PECon 2008), IEEE 2nd International, DOI: 10.1109/PECON.2008.4762468, 2008.
[31] V. Yilmaz, O. Turksoy, A. Teke, Improved PPT method to increase accuracy and speed in photovoltaic systems under variable atmospheric conditions, Int. J. Electr. Power Energy Syst. 113 (2019) 634–659.
[32] Y. Yang, H. Wen, Adaptive perturb and observe maximum power point tracking with current predictive and decoupled power control for grid-connected photovoltaic inverters, in: Journal of Modern Power Systems and Clean Energy, vol 7, 2019, pp. 422–432.
[33] M. Takruri et al., Support vector machine for photovoltaic system efficiency improvement, in: Journal of Sustainable Development of Energy, Water and Environment Systems, in press, doi: http://dx.doi.org/10.13044/j.sdewes.d7.0275, 2020.
[34] Padmanaban et al., A novel modified sine-cosine optimized MPPT algorithm for grid integrated PV system under real operating conditions, in: IEEE Access, vol 7, pp. 10467–10477, 2019.
[35] S. Silva et al, Feed-forward DC-bus control loop applied to a single-phase grid-connected PV system operating with PSO-based MPPT technique and active power-line conditioning, IET Renew. Power Gener. 11 (2017) 183–193.